Integrating Nonlinear Aerodynamic and Structural Analysis for a Complete Fighter Configuration

Kenneth E. Tatum*
Planning Research Corporation, Hampton, Virginia
and
Gary L. Giles†
NASA Langley Research Center, Hampton, Virginia

The coupling of a nonlinear aerodynamics program with a structural analysis program to include the effects of static aeroelasticity in early design studies is described. A nonlinear, full potential aerodynamics method with the capability to model geometric details of a complete aircraft in supersonic flow is used. The deflections of the lifting surfaces are calculated using an equivalent plate structural representation, which can readily accommodate the changes in stiffness and geometric properties required during early stages of the design process. An iterative solution procedure is used to obtain consistent aerodynamic loads and structural deflections at the specified flight conditions. The volume of data transmitted between programs is minimized. The procedure is applied to a complete aircraft, and the numerical results illustrate the aeroelastic effects on pressure distribution as well as total forces and moments. During this design study, the thickness distribution of the wing cover skins was initially sized based on rigid loads and subsequently resized under aeroelastic loads. Comparisons are made between these nonlinear aeroelastic results and results obtained from linear aerodynamic methods applied to a rigid shape during conceptual design studies.

Introduction

RECENT developments and improvements in computational methods, especially computational fluid dynamics (CFD), provide significantly improved capability to generate detailed analysis data for the use of all disciplines involved in the evaluation of a proposed aircraft design. Even greater benefits from these new technologies will be realized as they are integrated to account for interactions or couplings between disciplines and are extended and tailored for use as design tools.[1,2] These design tools could provide the sensitivity of overall performance characteristics to design changes proposed by the individual disciplines. Use of such information by designers, in conjunction with numerical optimization methods, could lead to greatly improved levels of efficiency and/or performance of advanced aircraft.

One beneficial use of integration is the inclusion of the effects of static aeroelasticity early in the design process.[2] Previous work[3] demonstrated such an integration method on a simplified wing-alone geometry. Other aerodynamic/structural integration efforts have employed linear aerodynamics, e.g., Ref. 4, primarily due to the computing requirements of advanced nonlinear CFD codes.[5,6] A few efforts have coupled nonlinear aerodynamic methods with finite-element structural analyses.[7,8] The current effort uses a simplified structural model which has the advantages of reduced model generation time and ease of design changes, and is readily interfaced to aerodynamics programs.

This paper describes one step in the development of an efficient method for computing the effects of aeroelasticity on the aerodynamic and structural characteristics of an aircraft design. The method integrates nonlinear aerodynamic theory and structural analysis in such a way as to be useful very early in the design process. The resulting design tool computes the aeroelastic deformation of the flexible wing structure under static loads and the corresponding effects on drag and pitching moment. A nonlinear, full potential aerodynamics method with the capability to model geometric details of a complete aircraft in supersonic flow is used. The deflections of the lifting surfaces are calculated using an equivalent plate structural representation which has the advantages of reduced model generation time and ease of design changes, as desired during early design studies. An iterative solution procedure is used to obtain consistent aerodynamic loads and structural deflections at the specified flight conditions, and the volume of data transmitted between programs at each iteration is minimized.

The method is intended to provide an assessment of static aeroelastic effects in very early stages of the design process when the definition of the conceptual design configuration is being refined. Aeroelastic considerations are usually not included in the conceptual design phase, and the method herein has potential to improve the quality of the design data and the resulting configuration during the early stages of design. As the design evolves and a detailed finite-element structural model becomes available, these calculations would be repeated using the improved representation of the structure. The converged aerodynamic loads and structural deflections obtained using the equivalent plate representation could be used to initialize the aeroelastic iteration process which includes the finite-element model.

The procedure is applied to a complete aircraft, and numerical results are presented to illustrate the aeroelastic effects. To illustrate the procedure's usefulness in early stages of design, the wing cover skins are resized to account for reductions in stress levels resulting from aeroelastic deformations. Comparisons are made between these nonlinear aeroelastic results and results obtained from linear aerodynamic methods applied to a rigid shape during conceptual design studies.

Received Sept. 11, 1987; presented as Paper 87-2863 at the AIAA/AHS/ASEE Aircraft Design, Systems and Operations Meeting, St. Louis, MO, Sept. 14-16, 1987; revision received June 28, 1988.

*Engineering Specialist. Member AIAA.
†Senior Research Engineer, Interdisciplinary Research Office, Structures Directorate. Associate Fellow AIAA.

Test Configuration

A previous study utilized a simple wing-alone geometry to demonstrate the process of coupling a nonlinear potential flow analysis code and a simplified structural analysis code for a specific design purpose.[3] The present study needed a configuration which would demonstrate the applicability of the methods to realistic geometries, e.g., a complete fighter aircraft. The aircraft chosen needed to provide some complexity without introducing difficulties which would detract from the research goals of the study.

A conceptual drawing of the aircraft selected is shown in Fig. 1. The design incorporates many advanced technologies, including the concept of Thrust Vector Control (TVC). The TVC aircraft is a tailless, twin-engine vehicle utilizing multiaxis thrust vectoring for directional control and trim at supersonic speeds, both in cruise (Mach = 2.0) and maneuver. The leading and trailing-edge devices are intended for subsonic maneuver, takeoff, and landing only.

This aircraft previously has been chosen as a testbed for an ongoing multidisciplinary research effort. The configuration is the result of conceptual design studies, and only limited experimental data for the aircraft exists, all for the rigid-body case. Experimental aerodynamic data for both the rigid and deformed shapes would be desirable for comparison with calculated data. The combination of a moderate-to-high wing loading for modern fighters and a relatively thin wing provided the potential for significant aeroelastic effects. Also, the use of thrust vectoring, instead of a horizontal tail, for trim and control eliminated the difficulties of analyzing multiple lifting surfaces, a problem inherent in many current production CFD codes. The simplicity of description coupled with potentially large physical effects made the TVC aircraft a desirable testbed for the current study. The TVC aircraft geometry is maintained at NASA Langley in a configuration geometry data base which provides a common geometry for both structural and aerodynamic analysts. A wireframe drawing of the discrete model is shown in Fig. 2 to illustrate the level of detail in this geometric representation.

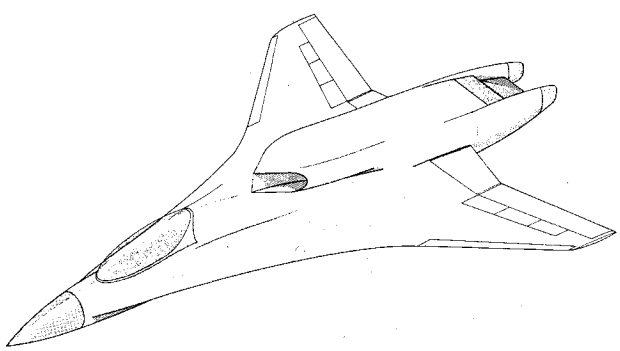

Fig. 1 Artist's conception of a TVC aircraft.

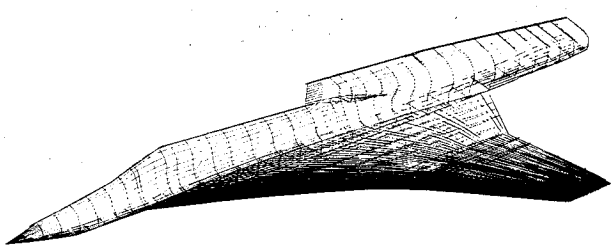

Fig. 2 Half-span wireframe drawing of the TVC aircraft; discretized data base model.

Aerodynamic Analysis Method

As noted previously, the aim of the current research was expanding the range of applicability of aero/structural coupling through the addition of nonlinear aerodynamic calculations on a complete aircraft. Previous work[3] used a version of nonconical relaxation (NCO-REL),[10] which was limited to a wing-alone geometry. The aerodynamic tool currently chosen is the SIMP code developed at Rockwell International Science Center for supersonic analysis of complex three-dimensional configurations. SIMP has been released to Computer Software Management and Information Center (COSMIC) as a production code, and a user's manual has been published.[11]

The SIMP (supersonic implicit marching program) code solves the steady-state form of the nonlinear full potential equation in conservation law form. The method couples the theory of characteristic signal propagation, flux biasing concepts, and body-fitted grid mapping procedures to compute efficiently steady supersonic flowfields about complex full aircraft configurations. The code has the capability to predict oblique shock waves and embedded subsonic pockets. Geometric features of multiple lifting surfaces, flow-through nacelles, and both yaw and angle of attack can be represented. In addition, graphic preand postprocessors are available for manipulating the geometry files, adjusting the grids, and plotting the SIMP output.

The geometry input to SIMP consists of a number of planar cuts through the aircraft, normal to the longitudinal (body) axis, consecutively defined from nose to tail, as shown in Fig. 3. On each of these planes discrete points define the body surface coordinates. Only a single body is allowed; therefore, aircraft components (i.e., fuselage, wing, tail, etc.) are not considered independently but collectively. Artificial wake cut definitions may be required to maintain this single-body definition aft of swept trailing edges. A geometry preprocessor[12] was used in conjunction with various splining techniques to generate the planar SIMP input cuts from the basic wireframe model.

SIMP employs a streamwise marching scheme to integrate the potential flow equation on successive planes, as shown in Fig. 3. A conical flow similarity solution is generated to start the calculation on a plane near the nose of the aircraft, which is assumed to be sharp, thereby allowing an attached bow shock wave (no embedded subsonic pocket). This starting solution defines the incoming flow for the next plane, a small step downstream. By repetitively stepping (marching) from one plane to the next, the entire length of the body is traversed. On each plane, a two-dimensional grid (Fig. 4) is constructed about the body, on which a finite-difference approximation to the flow equation is solved for the potential Φ. Tangential flow boundary conditions are applied on the body surface and freestream conditions are assumed at the outer grid boundary, with the expanding bow shock captured in between as part of the solution. The gradient of Φ is calculated by finite differences and used to compute velocity, density, and pressure at grid nodal points. Thus, at each longitudinal station down the body surface the flow variables, such as pressure, are computed at discrete node points both on the body surface and off the surface in the flowfield.

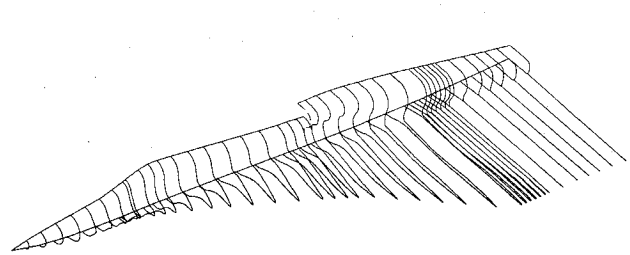

Fig. 3 SIMP input model of the TVC aircraft; baseline cruise geometry.

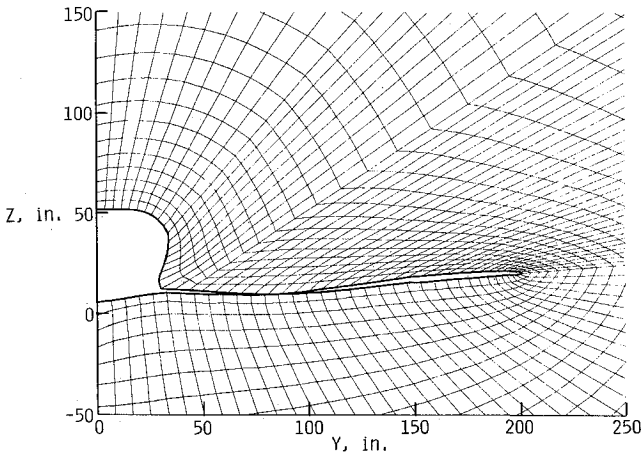

Fig. 4 Sample two-dimensional cross-plane grid generated by SIMP.

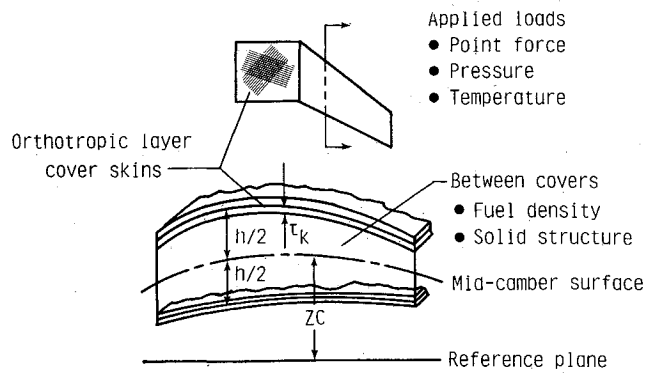

Fig. 5 Analytical representation of wing-box structure.

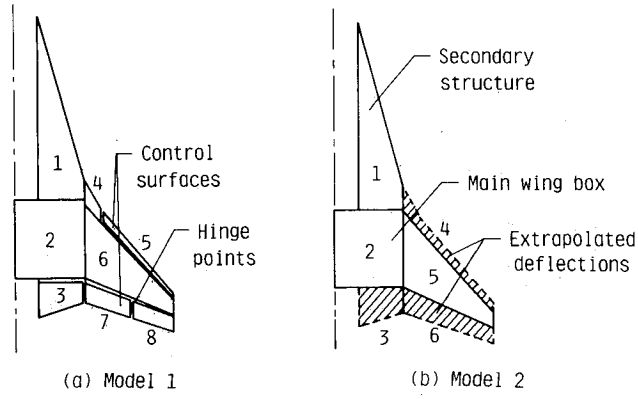

Fig. 6 Multiple plate segment models of the TVC wing structure.

Because of the marching nature of the SIMP solution procedure, each analysis is totally independent of other analyses. The solutions consist of complete sweeps from the conical nose approximation to the aircraft tail. Solution algorithms that are not single-sweep marching schemes may have the option to initialize the flowfield based on previously converged solutions at similar conditions; however, SIMP does not.

Although SIMP is quite versatile with respect to complex geometries, the wedge-shaped inlet of the TVC aircraft could not be modeled exactly within the current production code. Code within SIMP might be modified to allow such an inlet to be simulated through the boundary conditions, however, the simpler option of modifying the inlet face was chosen for this study. The modified face was defined to be flat at the longitudinal location where the true inlet was fully formed. The fuselage cross-sectional area at location and the true inlet capture area were maintained, however. Figure 3 shows the TVC geometry as actually input to SIMP. Note the multiple definitions at the inlet location and the inclusion of a zero-thickness wake downstream of the wing trailing edge.

Aerodynamic analysis codes employing Euler or Navier-Stokes theories eventually should replace SIMP and its attendant full potential theory in the overall methodology as they become cost effective. The interpretation of "cost effective" must be made by the design organizations who are evaluating the alternative codes. The CFD code selected must satisfy the practical limitations imposed by budget and calendar time available for the design studies since multiple aerodynamic analyses are required for each aeroelastic solution (see Interface Methodology section). Such future codes would embody fewer theoretical assumptions and, thus, more accurately describe the true physical flowfield. This future goal has been taken into account and the coupling makes no assumption on the nature of the aerodynamic theory, the calculation method used, or the type of computer required. The specific information passed between aerodynamic and structural modules has been kept minimal and will be described in a later section of the paper.

Structural Analysis Method

The structural analysis method used for this study is implemented in a computer program referred to as ELAPS (Equivalent Laminated Plate Solution).[9] This method requires only a small fraction of the volume of input data compared to a corresponding finite element structural model. The resulting reduction in numerical model preparation is important during early stages of design where many candidate configurations are being assessed. The wing structure is represented as an equivalent plate in this formulation, similar to the model for the symmetric cross-section wing-alone configuration of Ref. 3. The wing for the TVC configuration has both twist and camber so that the more general procedure discussed in Ref. 9 is required for structural modeling. The planform geometry of the structural box is defined by multiple trapezoidal segments, as shown by the two-segment box in Fig. 5. The cross-sectional view of a typical segment in Fig. 5 illustrates the analytical modeling of the wingbox structure. The wing depth h, camber definition zc, and cover skin thicknesses t are all defined in polynomial form over the planform of a segment. The geometry of the aerodynamic configuration is defined by the location of a set of discrete points, so that surface fitting procedures are required to determine the corresponding polynomial definition for the depth and camber used for the structural model.

The Ritz method[13] is used to obtain an approximately stationary solution to the variational condition of the energy of the structure and applied loads. In this method, the wing deflection is assumed to be represented in polynomial form as given for the bending deflection by

$$W = C_{00} + C_{10}x^1 + C_{20}x^2 + C_{01}y + \ldots + C_{mn}x^m y^n \qquad (1)$$

The Ritz solution is used to determine the numerical values of the set of unknown coefficients C_{mn}, that minimize the total energy. The solution, given in Eq. (1), provides a continuous functional definition of the wing deflection over the planform. This continuous definition expedites the interface of the structural and aerodynamic calculations.

The fuselage structure is assumed to be rigid in this study. The structural deflections of the wings change the distribution of aerodynamic pressures and the resultant lift force for a given aircraft angle of attack. These effects are considered in the aeroelastic calculations. Two different levels of modeling which could have been used to represent the wing structure are shown in Fig. 6. The equivalent plate analysis method has been extended to provide for modeling with multiple plate segments which can have separately defined displacement functions. The planform of model 1 is divided into eight segments: segments 2 and 6 represent the main wing box, segments 1 and 4

represent the secondary structure, and segments 3, 5, 7, and 8 represent the leading- and trailing-edge control surfaces. The control surfaces are attached to the main wing box by translational and rotational springs located at the hinge points, as shown in Fig. 6a.

In this study, thrust vectoring is used to trim the aircraft in a symmetric pull-up maneuver. The use of aerodynamic control surfaces for this purpose was not investigated and, therefore, model 2 was used in which the assumed displacement functions for the main structure were extrapolated into the leading- and trailing-edge areas, as indicated in Fig. 6b.

Interface Methodology

The flow conditions addressed in this paper are supersonic cruise and maneuver, where linear aerodynamic theory is often inadequate or, at best, limited by many assumptions and geometric restrictions. The present study acknowledges the cost of nonlinear aerodynamics, but explores the benefits of increased range of applicability afforded by nonlinear CFD and takes advantages of a new structural analysis tool[9] to reduce the total aero/structural computational effort. The two computational methods were coupled with as little modification as to the specific computer codes possible. Two major reasons exist for this philosophy:

1) To lessen the need for the designers to have intimate knowledge of all of the computer codes used, and

2) To allow the substitution of new analysis codes for the current ones, as they become available, without undertaking an entirely new integration effort.

For these reasons, all interface codes have been written in a very modular fashion. The practical considerations of efficient data transfer through these interfaces are addressed in this section.

A flowchart of the iterative procedure to arrive at the aeroelastically deformed shape of a wing at a specified flight condition is shown in Fig. 7. This procedure is described in Ref. 3, where the method was demonstrated for a simple wing-alone configuration. The conceptual design geometry, assumed to be that of the flexible aircraft at cruise, is used to begin the analysis. This baseline shape is analyzed at cruise to yield the jig (fabrication) shape, and at maneuver for an initial estimate of the elastic maneuver loads. Application of these maneuver loads to the jig shape produces an initial approximation of the elastic maneuver shape. Iteration proceeds by computing loads on the current maneuver shape approximation and applying these loads to the jig shape. At each aerodynamic load analysis the maneuver lift is maintained by adjusting the aircraft angle of attack. Convergence is achieved when the calculated airloads are consistent with the structural deflection from the jig shape. In practice, the convergence test is that the shape change between iterations is less than some tolerance.

This iterative procedure requires the passing of aerodynamic load data from aerodynamics to structures and wing geometry deformations from structures to aerodynamics. In order for the procedure to be useful in early stages of design, it is important to expedite this data transfer.

The ELAPS structural code greatly simplifies the aerodynamics-to-structures data transfer. A NASTRAN or engineering analysis languages (EAL) finite-element model requires the air-loads to be applied at structural nodes which, in general, are not identical to the aerodynamics nodes. Surface interpolation schemes are required to integrate the pressures and compute airloads at the appropriate locations. When the interpolation is done within the aerodynamics code, the details of an often complex structural model must be available along with the aerodynamic model description, both typically consisting of large data bases. When the interpolation is performed within the structures code, a large data file of pressures and three-dimensional coordinates must be saved from each aerodynamic analysis. Another approach is to create an intermediate code with access to both the structural nodal

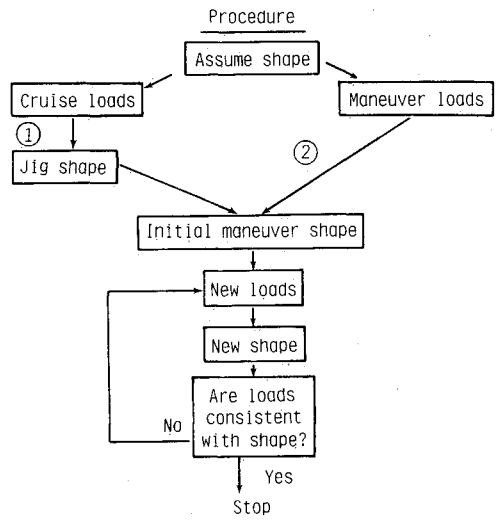

Fig. 7 Flexible wing aerodynamics/structural analysis procedure.

geometry and the aerodynamic loads data. This approach increases the time required for each structural/aerodynamic iteration. For any of these approaches, care must be taken to avoid introducing waves in the load distribution caused by interpolation, particularly in the vicinity of shock waves. The analytic formulation of ELAPS allows the load distribution to be applied at the aerodynamic nodes, thus eliminating the interpolation step required for finite-element structural analysis. An equivalent load vector corresponding to the number of unknown displacement function coefficients [Eq. (1)] is required for analysis of the equivalent plate structure. This load vector is formed by integrating the product of point forces and displacement function terms.

Numerical integration to provide this load data for ELAPS has been easily incorporated into SIMP with minor coding changes. The only structural information required by the aerodynamics code is the planform geometry of each equivalent plate segment (six numbers per segment). A single subroutine, added to the SIMP code, is called each time a set of pressures is obtained. This subroutine requires the grid point coordinates, directional pressure components, and the finite difference area over which the discrete pressure is applied; all information already computed within SIMP (and most other CFD codes). The subroutine searches for the correct structural panel and cumulatively integrates the products of pressure coefficients and areas with each polynomial term of Eq. (1) as required by ELAPS. At SIMP termination, when all pressures have been integrated, a relatively short file is output containing the segment geometries and the total pressure integrals, typically on the order of 100 numbers per segment. This quantity depends on the number of displacement function terms used for structural analysis. The time requirement for this load integration is only 1 or 2% of the total SIMP execution time. The only modifications to SIMP were two lines of code appropriately placed to call the added subroutines (one to perform integration and one to write out the data file). These added routines were written to require minimal modification in order to be incorporated into other CFD codes.

The transfer of data from structures to aerodynamics involves similar considerations to those just described. ELAPS processes the aerodynamic load information to determine structural deflections in the form of continuous polynomials as functions of spanwise and chordwise location within each equivalent plate segment. These continuous, analytic definitions of displacements can be evaluated at each point of the aerodynamic input geometry and used directly to generate a deformeds configuration.

As in the aerodynamics-to-structures transfer, several options exist as to where the deformed wing geometry should be calculated. Because of the size and unique formats of nonlin-

ear CFD input files, it was not desirable to locate the calculations within ELAPS. They could be embedded within SIMP, as for the aerodynamics-to-structures transfer, but the interest in visualizing the deformed geometry relative to the baseline indicated the usefulness of an intermediate program. Along with computer graphics, the program involves only simple calculations: 1) search for the appropriate structural segment, and 2) evaluation of a simple polynomial expression [Eq. (1)]. The only inputs are the baseline SIMP input geometry and the polynomial coefficients for cruise and maneuver as calculated from ELAPS; again, approximately 100 numbers per segment are passed between the disciplines. Also, after execution of this intermediate program, record of the geometry is saved at each step of the aeroelastic iteration, which allows convergence to be verified visually. As indicated previously, the wing structural model need not be identical with the aerodynamic model. The equivalent plate planform of the TVC wing was shown in Fig. 6b. Aerodynamic loads were computed on each of the six plates shown, however, the structural model was chosen to include only the principal wing structure, plates 1, 2, and 5. Plates 3, 4, and 6 are primarily flaps and ailerons, and their loads were combined to yield net effects on the main wing structure. Displacements of these additional plates were determined by extrapolation of the polynomial displacement functions of the primary plates.

Displacement function extrapolation was also necessary to maintain continuity of the aerodynamic wake/wing model. This extrapolation down the wake has no structural significance; the aerodynamic wake boundary condition is that of zero load on the fictitious wake surface (vortex sheet). However, the SIMP input geometry requires continuous section definitions; therefore, the wake must be allowed to float up or down with the elastic wing trailing edge. To prevent the extrapolated function from growing unbounded far downstream the polynomial is multiplied by a damping function that is unity at the wing trailing edge and fuselage side, and decreases outboard and downstream. For the current study, the damping function was chosen as a product of two functions: 1) a cubic function of streamwise distance from the trailing edge, and 2) a bilinear function of span and streamwise distances. This definition is not unique, however, and was determined by numerical trial and error. Two free parameters in the definition allow the user to vary the rate of damping.

Results

The procedure was applied to the TVC aircraft at two different loading conditions. The primary mission for the TVC is one of high-altitude interdiction. The ultimate maneuver criteria of an 8.1-g load factor at Mach 2 and 40,000-ft altitude were chosen as the primary test case. A lower load factor of 2g at the same Mach number and altitude was selected for the second test case. The aircraft was designed to cruise at Mach 2 and 65,700 ft. Using these criteria and the conceptual design estimates of the vehicle weight, payload, and fuel capacities, the cruise lift coeficient C_L was determined to be 0.19. The two maneuver lift coefficients were estimated at 0.361 and 0.089 for 8.1 and 2g, respectively. Nonlinear aerodynamic analyses of the rigid geometry were performed for these three values of lift coefficient. These analyses required several preliminary runs to determine the relationship between C_L and the angle of attack since direct-analysis CFD codes require angle of attack as input, while lift coefficient is an output.

Comparisons of forces and moments at Mach 2 are presented in Fig. 8 as predicted by 1) linear aerodynamic analysis of rigid aircraft, 2) nonlinear aerodynamic analysis of rigid aircraft, and 3) nonlinear aeroelastic analysis of flexible aircraft. At low lift, the differences of these results are small, indicating the applicability of linear, rigid aerodynamic theory for conceptual design in the low-lift range. At high values of lift coefficient, the differences in drag and moment are more pronounced. These differences should be measured at constant lift (along the horizontal direction) and not normal to the

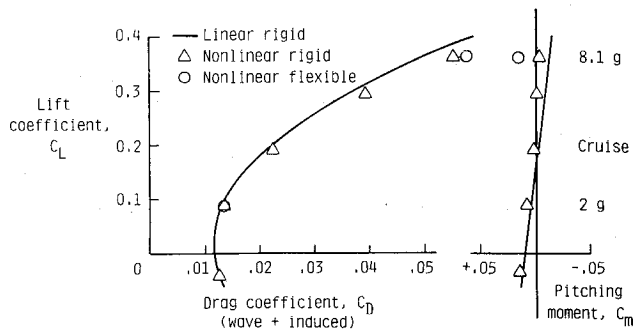

Fig. 8 Aerodynamic force and moment predictions for the TVC aircraft at Mach 2.

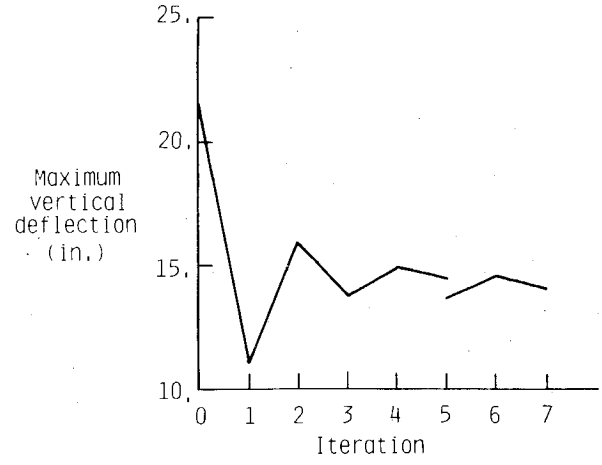

Fig. 9 Aeroelastic iteration history for wing 1; Mach 2, 8.1-g maneuver load factor.

curves since the maneuver load factor specifies the required lift. The high-lift results will be discussed further in the following paragraphs.

The aeroelastic iteration for the 8.1g load case produced an oscillatory convergence pattern, as illustrated in Fig. 9. The iteration history of maximum computed deflection of the wing structural box, under the maneuver loads, is shown. The maximum was consistently at the tip trailing edge of the outboard structural plate. The initial (zeroith iteration) deflection is due to loads on the rigid cruise shape analyzed at the angle of attack, which gives the maneuver lift coefficient. The twist-due-to-load angle of attack required to maintain lift, drag coefficient C_D, and pitching moment coefficient C_M all exhibited the same oscillatory behavior, although not all quantities were in phase.

Figure 9 illustrates the first test of the SIMP/ELAPS aeroelastic coupling. The iteration was stable and convergent, and no relaxation of either deflections or loads was required. In later aeroelastic analyses, the change in deflections was underrelaxed by a factor of 0.75 in an attempt to damp out the oscillations. The underrelaxation appeared to accelerate the convergence slightly but was not essential for this particular structure.

As a preliminary design analysis, the change after five iterations was considered negligible and the iteration was stopped. Net effects of static aeroelasticity were computed to be $\Delta C_D = +0.0019$ and $\Delta C_M = +0.0194$. The maximum deflection (from the baseline cruise geometry) was 15.82 in. at the wingtip trailing edge (7.8% of the semispan). The loading caused the wing to twist 4.8 deg, leading edge down. The five iterations required six individual aerodynamic analyses in addition to the baseline cases. The initial relationship between lift coefficient and angle of attack had to be updated because it

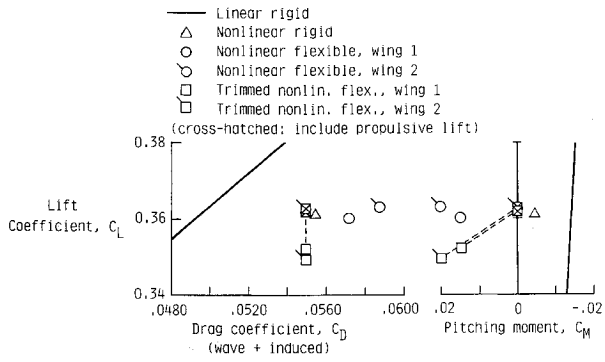

Fig. 10 Aerodynamic force and moment predictions for the 8.1-*g* maneuver load factor at Mach 2.

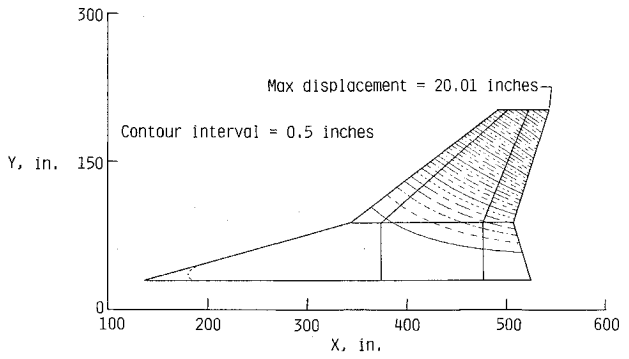

Fig. 11 Contours of computed structural displacements on wing 2; Mach 2, 8.1-*g* maneuver load factor, trimmed.

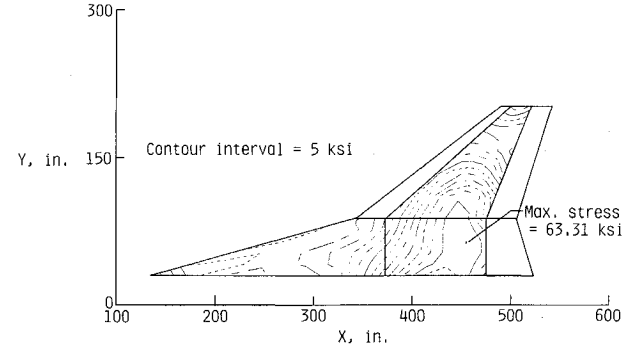

Fig. 12 Contours of computed spanwise stress components on wing 2; Mach 2, 8.1-*g* maneuver load factor, trimmed.

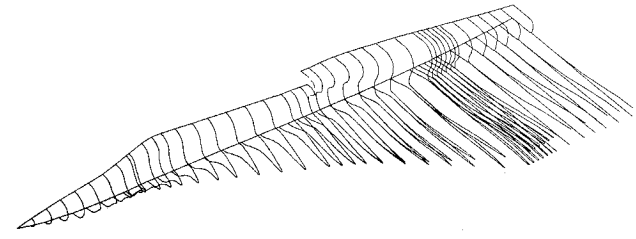

Fig. 13 Overlay of rigid and deformed geometries for wing 2; Mach 2, 8.1-*g* maneuver load factor, trimmed.

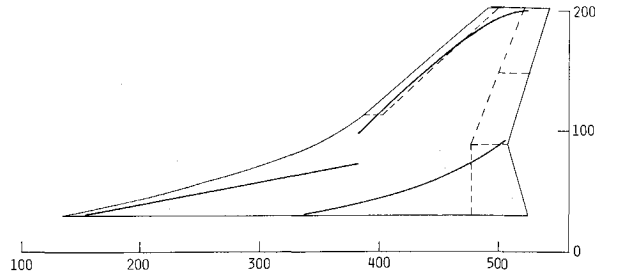

Fig. 14 Computed upper wing surface shock-wave pattern; Mach 2, 8.1-*g* maneuver load factor.

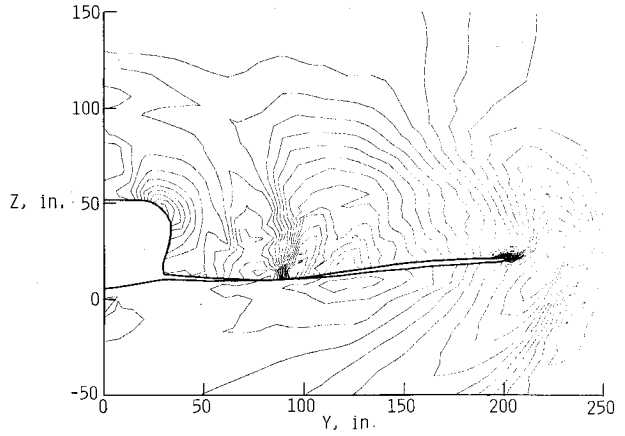

Fig. 15 Cross-plane pressure contours about deformed wing 1; Mach 2, 8.1-*g* maneuver load factor, X = 503.5 in.

changed slightly as the geometry deflected, and an additional aerodynamic analysis was used to estimate this change.

The aeroelastic solution described earlier does not include the effects of trim. The large positive moment generated by the deflected wing is noticeably different from the conceptual design prediction of small negative moment. In this study the aircraft was trimmed by vectoring the thrust of the engine. Use of thrust vectoring for trim allowed the geometry to be a function only of loading, not flap settings. The trim force was represented as the vertical component of thrust at the mean location of the nozzle vanes.

This trim force was introduced at iteration 5, as indicated by the discontinuity in the iteration history of Fig. 9. Using the converged aeroelastic C_M, the initial trim force, and resulting lift increment, was computed. Subtracting this ΔC_L (a propulsive lift increment) from the desired maneuver lift yielded the lift contribution required from aerodynamic forces, C_l^{aero}. The deformed geometry obtained from the first five iterations was analyzed at this new lift coefficient and the aeroelastic iteration was continued. However, at each aerodynamic analysis, the trim force was recomputed from the previous C_M and the desired C_l^{aero} was changed to maintain the total lift as before.

Three additional iterations were required to reconverge the aeroelastic analysis, including trim. Trim requirements, for the positive C_M, tended to relieve the aeroelastic effects: the maximum deflection reduced from 15.82 to 15.36 in. and twist due to load was reduced to 4.68 deg. More importantly, the drag was reduced by 0.0022 from the untrimmed aeroelastic solution.

Magnified views of the drag and moment diagrams are presented in Fig. 10 to illustrate more clearly the effects of nonlinearity and aeroelasticity. The solid line is the conceptual design prediction (linear, rigid) and the triangle is the nonlinear rigid analysis. The circles and squares are the results of aeroelastic analyses, untrimmed and trimmed, respectively. Cross-hatched symbols include the propulsive lift component due to thrust vectoring.

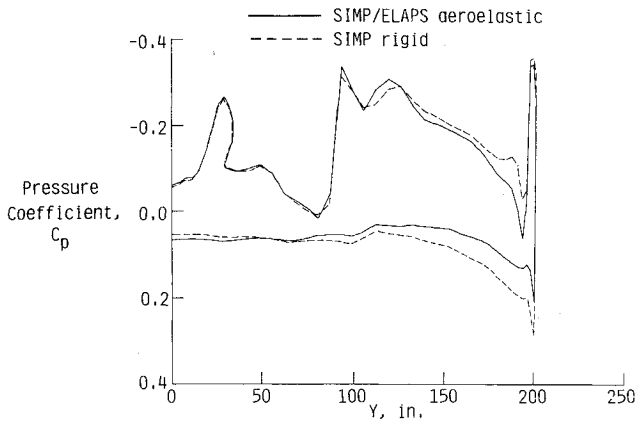

Fig. 16 Spanwise pressure coefficient distributions on rigid and deformed geometries for wing 1; Mach 2, 8.1-*g* maneuver load factor, $X = 503.5$ in.

During this design study, the thickness distribution of the wing cover skins was sized initially using loads on the rigid cruise shape at the 8.1-*g* load factor. The deflection, calculated in the aeroelastic analysis, of this first structural model, herein referred to as wing 1, caused an inboard shift of the aerodynamic pressures and a corresponding reduction in stress levels in the cover skins. The thickness of the wing skins was then resized using the 8.1-*g* aeroelastic loads. This wing with resized (reduced thickness) skins, referred to as wing 2, was more flexible than wing 1 and required subsequent aeroelastic analysis. The flagged symbols in Fig. 10 show the same aeroelastic analysis procedure applied to the resized structural model, wing 2.

The converged structural aeroelastic effects at an 8.1-*g* load factor for wing 2, including trim effects, are illustrated by Figs. 11–13. Contours of deformation from the cruise geometry are shown over the entire exposed wing planform in Fig. 11. Figure 12 plots contours of spanwise stress components over the exposed wing structural box. An oblique view of the entire deformed SIMP geometry superimposed on the cruise geometry in Fig. 13 further illustrates the structural deformation caused by aeroelastic loading.

Despite the large structural deflection at 8.1*g* and the large shift in moment, the aerodynamic flowfield did not change substantially. The upper-surface shock pattern (illustrated in Fig. 14) did not change noticeably in any of the high-lift cases, either rigid or elastic. The highly oblique shocks tended to be strong functions of planform and inlet location rather than the wing deformation. A sample cross-plane pressure contour plot is given in Fig. 15 for the deformed (untrimmed) wing 1, showing the oblique inlet shock wave near $Y = 100$.

This inlet shock is also prominent in the spanwise pressure plot of Fig. 16, along with the leading-edge shock, which potential theory tends to predict. The unloading of the wing tip due to flexibility is illustrated by comparison of the pressure distribution of the elastic and rigid geometries at the same lift (wing 1, untrimmed) for a sample longitudinal station. Again, the shock locations are identical; only the shock strengths are changed. The computational grid generated at this particular body station for the untrimmed elastic geometry was shown in Fig. 4.

Concluding Remarks

A general method for integrating a nonlinear computational aerodynamic analysis method with an equivalent plate structural analysis method has been described and applied to a complete aircraft. The method was developed as a tool for early design studies, thereby incorporating both nonlinear aerodynamic effects, such as shock waves, and flexibility effects early in the overall design cycle. The use of a simplified structural method allows an early estimate of aeroelastic effects to be made before a detailed finite-element model becomes available. The resulting data can be used to improve the quality of the conceptual design configuration.

A state-of-the-art production computational fluid dynamics code, SIMP, was selected to perform the aerodynamic analysis. SIMP was chosen based on cost, accuracy, geometric flexibiliy, and production code status, and no particular endorsement of potential flow theory was intended. The current set of codes constitutes but one stage in the development of an accurate preliminary design tool. As cost-effective, production CFD codes for complete aircraft based on the Euler and Navier-Stokes equations become available, they should replace SIMP within the aeroelastic procedure. In view of this objective, all couplings between aerodynamic and structural modules have been written in very generic code; i.e., little or no dependence on the characteristics of a particular CFD program.

A complete fighter aircraft has been analyzed for static aeroelastic effects using the procedure and analysis modules described in this paper. To illustrate the procedure's usefulness as a tool during structural sizing, an initial wing structure was analyzed and subsequently resized when the computed stresses were found to be well within design limits.

References

[1]Tolson, R. H. and Sobieszczanski-Sobieski, J, "Multidisciplinary Analysis and Synthesis: Needs and Opportunities," AIAA Paper 85-0584, April 1985.

[2]"Static Aeroelasticity in Combat Aircraft,"AGARD Rep. 725, Jan. 1986.

[3]Pittman, J. L. and Giles, G. L., "Combined, Nonlinear Aerodynamic and Structural Method for the Aeroelastic Design of a Three-Dimensional Wing in Supersonic Flow," AIAA Paper 86-1769, June 1986.

[4]Caap, P. and Elmeland, L., "Calculation of Static Elastic Effects on a Modern High Performance Fighter Aircraft," *Proceedings of the AIAA 4th Applied Aerodynamics Conference,* AIAA, New York, June 1986.

[5]Jameson, A., Baker, T. J., and Weatherill, N. P., "Calculation of Inviscid Transonic Flow over a Complete Aircraft," AIAA Paper 86-0103, Jan. 1986.

[6]Vadyak, J., "Simulation of Wing, Fuselage, and Wing/Fuselage Flowfields Using a Three-Dimensional Euler/Navier-Stokes Algorithm," AIAA Paper 85-1693, July 1985.

[7]Whitlow, W., Jr. and Bennett, R. M., "Application of a Transonic Potential Flow Code to the Static Aeroelastic Analysis of Three-Dimensional Wings," AIAA Paper 82-0689, May 1982.

[8]Campbell, R. L., "Calculated Effects of Varying Reynolds Number and Dynamic Pressure on Flexible Wings at Transonic Speeds," NASA CP-2327, Vol. 1, April 1984, pp. 309–327.

[9]Giles, G. L., "Further Generalization of an Equivalent Plate Representation for Aircraft Structural Analysis," *Proceedings of the AIAA/ASME/ASCE/AHS 28th Structures, Structural Dynamics and Materials Conference,* AIAA, New York.

[10]Siclari, M. J., "Supersonic Nonlinear Potential Flow Analysis – Interim Rept.," NASA CR 172456, Aug. 1984.

[11]Shankar, V., Szema, K.Y., and Bonner, E., "Full Potential Methods for Analysis/Design of Complex Aerospace Configurations," NASA CR 3982, May 1986.

[12]Hall, J. F., Neuhart, D. H., and Walkley, K. B., "An Interactive Graphics Program for Manipulation and Display of Panel Method Geometry," NASA CR 166098, March 1983.

[13]Langhaar, H. L., *Energy Methods in Applied Mechanics*, Wiley, New York, 1962.